URSI GASS 2020, Rome, Italy, 29 August - 5 September 2020

Embedded Element Patterns in Hierarchical Calibration of Large Distributed Arrays

Stefan J. Wijnholds
ASTRON, Dwingeloo, The Netherlands

Abstract

Large distributed aperture array systems like the Low Frequency Array (LOFAR) and the low-frequency component of the Square Kilometre Array (SKA-LOW) require calibration at station level and at array level. At both levels, use of a priori knowledge of the embedded element patterns (EEPs) of the antennas is needed. In this paper, I propose accuracy requirements for station calibration and absolute calibration of the synthesis array system and assess the level of detail needed in modelling of the EEPs (individual, average or isolated) to meet them.

1 Introduction

Large radio astronomical aperture array systems usually have a hierarchical design in which the receiving elements are grouped in *stations*, which together operate as an interferometer array. Examples of such systems are the Low Frequency Array (LOFAR) [1] and the low-frequency component of the Square Kilometre Array (SKA-LOW) [2]. Such systems require calibration at different aggregation levels to ensure high-quality scientific data products: station level calibration is required to form station beams with sufficient quality and stability, and array level calibration is required to meet the performance criteria for the interferometer array [3].

Antenna measurements using drones and developments in computational electromagnetics allow us to make validated predictions of the embedded element pattern (EEP) of individual antennas in such large arrays [4]. In this paper, I propose accuracy requirements for station calibration and absolute flux calibration of the interferometer array and assess the impact that EEP modelling errors have on these factors. Based on this assessment, I discuss the level of detail required in modelling of the EEPs (individual EEP for each antenna, average EEP for all antennas within a station or isolated element pattern for a single antenna) to meet the needs of LOFAR and SKA-LOW.

2 Station level calibration

The aim of station calibration is to keep track of electronic drift in the individual receive paths in the station due to, e.g., temperature variations and ageing of electronic components. This information is required to form a well-defined beam in the desired direction. Simulations have shown that the impact of ignoring EEP differences in the modelling of the intra-station visibilities causes a systematic error in the station calibration solutions that varies with sidereal time [5]. If these calibration solutions would be fed back to the beamforming system, the station beam would exhibit a drift-like effect even when the station electronics would be perfectly stable. I will refer to this as *calibration drift*. As the aim of station calibration is to improve system performance, calibration drift should be less than electronic drift, at least when direct feedback of station calibration solutions to the beamforming system is being considered. The combination of electronic drift and calibration drift gives rise to decorrelation in the station beamformer and to drift of the station beam(s) formed. Below, I provide derivations that can be used to set requirements such that these detrimental effects remain within acceptable limits.

The excitations of the individual elements of the array in response to a plane wave impinging on the array at a given frequency can be represented by phasors, whose phases describe the geometrical delay of the wave across the array w.r.t. a common reference point. If the beamformer works perfectly, all these phasors are aligned parallel before addition thereby maximising the amplitude of the desired signal. Based on this argument, it is easily seen that, for a reasonably small RMS phase error σ_φ, this will result in a vector that is only a fraction $\cos(\sigma_\varphi)$ of the length achievable by perfect addition. In the power domain, the beamformer efficiency given RMS phase errors σ_φ is therefore

$$\eta_{\mathrm{BF}} = \cos^2(\sigma_\varphi). \tag{1}$$

This implies that a beamformer efficiency of 99% requires $\sigma_\varphi \leq 5.7^\circ$ while a beamformer efficiency of 98% requires $\sigma_\varphi \leq 8.1^\circ$.

Although Eq. (1) is insightful, it does not set a limit on the inter-element amplitude variations. For this, we need to consider the output SNR of the beamformer,

$$\mathrm{SNR}_{\mathrm{BF}} = \frac{\mathbf{w}^H \mathbf{R}_{\mathrm{s}} \mathbf{w}}{\mathbf{w}^H \mathbf{R}_{\mathrm{n}} \mathbf{w}}, \tag{2}$$

where $\mathbf{w}$ is the vector with beamformer weights and $\mathbf{R}_{\mathrm{s}}$ and $\mathbf{R}_{\mathrm{n}}$ are the array covariance matrices for the signal and noise respectively [6]. Assuming a source of unit power in the

phase center ($\mathbf{R}_\mathrm{s} = \mathbf{1}\mathbf{1}^H$, where $\mathbf{1}$ denotes a vector filled with ones) and elements with unit noise power ($\mathbf{R}_\mathrm{n} = \mathbf{I}$, where $\mathbf{I}$ denotes the identity matrix), Eq. (2) simplifies to

$$\mathrm{SNR}_\mathrm{BF} = \frac{\mathbf{w}^H\mathbf{1}\mathbf{1}^H\mathbf{w}}{\mathbf{w}^H\mathbf{I}\mathbf{w}} = \frac{\left|\mathbf{w}^H\mathbf{1}\right|^2}{\mathbf{w}^H\mathbf{w}}. \tag{3}$$

This equation can be used to compare the output SNR of the beamformer for various error distributions against the output SNR of an error-free beamformer. As an example, I will assume beamformer weights with zero-mean Gaussian noise with standard deviation ε on its real and imaginary parts, i.e., $w_p = 1 + e_p^\mathrm{Re} + \mathrm{j}e_p^\mathrm{Im}$ with $e_p^\mathrm{Re,Im} \sim \mathcal{N}(0,\varepsilon)$, where p denotes the element index. This gives

$$\mathrm{SNR}_\mathrm{BF} = \frac{\left|\sum_p 1 + e_p^\mathrm{Re} - \mathrm{j}e_p^\mathrm{Im}\right|^2}{\sum_p 1 + 2e_p^\mathrm{Re} + \left(e_p^\mathrm{Re}\right)^2 + \left(e_p^\mathrm{Im}\right)^2}. \tag{4}$$

Since the errors are assumed to have zero mean, the linear error terms will vanish if the number of elements in the array, P, is sufficiently large. In the same limit, the quadratic term in the denominator will converge to $2P\varepsilon^2$. Taking into account that the ideal beamformer would have an SNR of P, the beamformer efficiency in this example becomes

$$\eta_\mathrm{BF} = \frac{\mathrm{SNR}_\mathrm{BF}}{P} = \frac{1}{1+2\varepsilon^2} \approx 1 - 2\varepsilon^2, \tag{5}$$

where the approximation for small errors is based on the Taylor series of $1/(1+x)$. This result implies that a beamformer efficiency of 99% requires $\varepsilon \leq 7.1\%$ while a beamformer efficiency of 98% requires $\varepsilon \leq 10\%$.

In theory, the station beams can be predicted based on a priori information like station beam weights, operational antennas and their EEPs. In practice, this prediction will not be perfect and array level calibration will have to handle deviations between the actual station beams and the predicted station beams. If this deviation is constant, long calibration intervals can be used in direction-dependent (DD) calibration to estimate this deviation very accurately. This task becomes more challenging when this deviation is varying with time. This issue can be analysed by considering the contribution of visibility V_{ij} to the imaging of a source with flux S at some point in the field-of-view towards which the stations involved have gains g_i and g_j when this contribution is integrated over the calibration time interval τ,

$$V_{ij} = \frac{1}{\tau}\int_{-\tau/2}^{\tau/2} \frac{g_i}{g_{0i}}\frac{\overline{g_j}}{\overline{g_{0j}}} S \mathrm{d}t, \tag{6}$$

where g_{0i} and g_{0j} are the calibration corrections applied.

Initially, the changes in the DD gains g_i and g_j will, to first order, be linear. Assuming that the calibration routine perfectly estimates the average value of the gains over the calibration interval, we can describe g_i as $g_i = g_{0i} + \alpha_i t$. The visibility is then described by

$$V_{ij} = \frac{1}{\tau}\int_{-\tau/2}^{\tau/2} \frac{g_{0i} + \alpha_i t}{g_{0i}}\frac{\overline{g_{0j} + \alpha_j t}}{\overline{g_{0j}}} S \mathrm{d}t. \tag{7}$$

Performing the integration gives

$$V_{ij} = S + \frac{1}{12}\frac{\alpha_i}{g_{0i}}\frac{\overline{\alpha_j}}{\overline{g_{0j}}}\tau^2 S = S + \Delta S. \tag{8}$$

If the bias due to drift of the station beam is uncorrelated between visibilities, drift effectively acts like another source of noise that we would like to keep below the thermal noise in the image. Keeping it below 20% of the thermal noise implies that

$$\frac{|\Delta S|}{S} \leq \frac{1}{5}\frac{\mathrm{SEFD}/\sqrt{B\tau}}{S} = \frac{1}{5}\frac{1}{\mathrm{SNR}}, \tag{9}$$

where SEFD refers to the Source Equivalent Flux Density of the system and SNR is the SNR of the source with flux S used for DD calibration.

Assuming that the drift rates follow a random distribution with RMS magnitude α and the true gains are nominally identical with magnitude g_0, Eq. (9) can be written as

$$\frac{1}{12}\frac{\alpha^2}{g_0^2}\tau^2 \leq \frac{1}{5}\frac{1}{\mathrm{SNR}}, \tag{10}$$

which implies a limit on the rate of change of the relative error on the directional response of the stations of

$$\frac{\alpha}{g_0} \leq \sqrt{\frac{12}{5}}\frac{1}{\sqrt{\mathrm{SNR}}}\frac{1}{\tau} = \sqrt{\frac{12}{5}}\sqrt{\frac{\mathrm{SEFD}}{S\sqrt{B\tau}}}\frac{1}{\tau}. \tag{11}$$

Calibration intervals are usually chosen such that the SNR towards the (clusters of) calibration sources is at least 5 to 10. To find a conservative estimate, I will assume an SNR of 10. In LOFAR, common solution intervals for calibration of DD instrumental effects are 5 to 10 minutes. To find a conservative estimate, I will assume 10 minutes, i.e., $\tau = 600$ s. These values give $\alpha/g_0 \leq 0.082$ %/s. For SKA-LOW, the allowed rate of change will be higher owing to its higher sensitivity. The lower SEFD implies that a shorter integration time is sufficient to perform DD calibration with the same density of directions and SNR. This relaxes the requirement, i.e., DD calibration is able to keep up with faster changing station beams.

The impact of ignoring EEP differences between antennas was assessed in simulation for a SKA-LOW station consisting of SKALA4AL antennas located at the AAVS site (-27.6° S, 116.7° E). Mock visibility data were created at 110 MHz based on the Haslam map [7] and individual EEPs from an EM-simulation validated by drone measurements [8]. For calibration, model visibilities were created based on the Haslam map assuming an identical EEP for all elements in the station equal to te average EEP from the EM-simulation. Calibration was performed for 200 instances in time spread over 24 hours starting at 22 August 2018 at 0:00:00 UTC. The estimated gains were applied to classical delay beamformer weights to calculate a station beam for each of the 200 instances. Fig. 1 shows the local relative station beam gain variations for a number of points

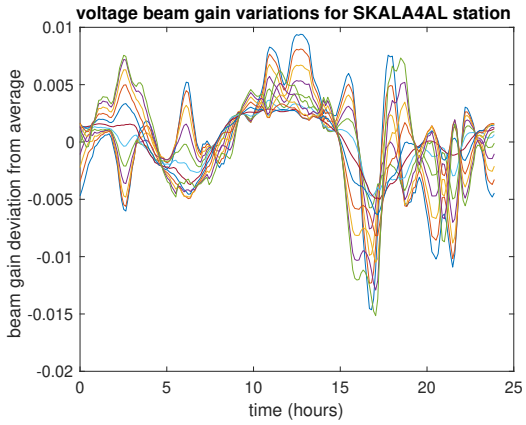

Figure 1. Local relative station beam gain variations along the cross-section through the main beam with largest variability as function of time since 22 August 2018, 0:00:00 UTC.

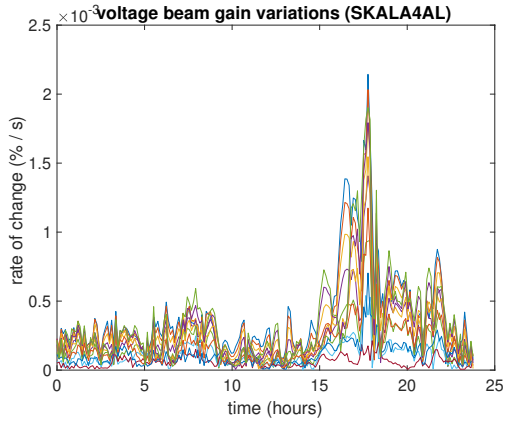

Figure 2. Rate of change of the local relative station beam gain variations shown in Fig. 1.

sampling the cross-section through the station main beam where the highest variability was found. By taking the difference between the station beam gain predictions for consecutive time instances, an estimate was calculated for the rate of change of the relative error. The results are shown in Fig. 2.

These results indicate that, although ignoring EEP differences in station calibration results in a bias, the rate of change of this bias is slow enough that continuous re-calibration of a station during an observation will not result in station beam variations at a rate of change that DD calibration at array level will not be able to deal with. Also, even at the most unfavourable instance in time, the RMS phase variation induced by this bias on the gain solutions for the individual receive paths within a station is expected to be less than 4°. This only causes 0.5% decorrelation in the station beamformer, which is well within the allowed budget for beamforming errors. We may thus conclude that a priori knowledge of an average EEP is sufficient for station calibration. In both simulation and experiments with LOFAR and the AAVS prototype station, we found, however, that errors in the currently used source model may cause an even larger bias than ignoring EEP variations. This needs to be validated carefully before opting for continuous re-calibration of the station during an observation.

3 Array level calibration

DD calibration is a pre-requisite for high-dynamic range imaging [9]. LOFAR Epoch-of-Reionization observations and, to a lesser extend, LOFAR survey observations therefore perform DD calibration in $\sim$10 to even $\sim$ 100 directions [10, 11]. DD calibration in LOFAR does not only provide ionospheric corrections, but also corrections for discrepancies between the station beam model and the actual station beam. As the station beam shape is mainly determined by the array factor, an inaccurate model of the EEPs of the antennas within a station is usually not a major issue if DD calibration is applied.

The EEPs play a more important role in flux calibration. For flux calibration, the telescope is pointed at a flux calibrator to establish the telescope gain shortly before or after the observation of the target field [11]. Unfortunately, the telescope gain of an aperture array varies significantly with pointing direction, mainly due to the (average) EEP and projection effects. As a result, the telescope gain towards the flux calibrator and towards the target field, which may be separated by $\sim$100° on the sky, may differ considerably and this needs to be taken into account during flux calibration transfer from the calibrator to the target field. This issue has been discussed extensively in the LOFAR project as plans are being made towards its upgrade to LOFAR 2.0. Considering that the absolute flux scale at 150 MHz is about 5% uncertain (Reinout van Weeren, private communication) and that flux calibration transfer should not significantly add to this, the system requirements for LOFAR 2.0 now specify that *"LOFAR 2.0 shall provide a flux calibration of sources with a reproducibility better than 2% independent of the sky position above an elevation of 10 degrees."* Here, reproducibility refers to the ability to reproduce the flux scale of the target field when using a different flux calibrator or performing flux calibration at a different sidereal time.

To meet this reproducibility target, we need to know the overall gain of the station in a given direction, i.e., the sum of all individual EEPs after phasing up towards the direction of interest, across the sky within 1.4% assuming that the errors towards the calibrator and towards the target field are unrelated and may therefore be added quadratically. Since calculation of the isolated element pattern (IEP) is much less computationally demanding than calculation of the average EEP (aEEP), the difference between the IEP and the aEEP was studied in detail for the LOFAR LBA system [12]. The results indicate that, for the relatively sparse LBA outer configuration of the Dutch LOFAR stations, the differences between the IEP and aEEP remain within the 1.4%

limit for boresight angles up to 60° at fiducial frequencies of 32, 44, 57 and 70 MHz. For the more densely packed LBA inner array, the situation is different. At 32 MHz, the requirement is met for boresight angles up to 60°. At 44, 57 and 70 MHz, however, the requirement is only met over a more restricted range of boresight angles, up to about 30°, 40° and 25° respectively. Therefore, a full EM simulation of an entire LOFAR station may be required to achieve the desired flux calibration reproducibility.

A similar analysis was done for an SKA-LOW station [13]. At 50 MHz, the difference between the IEP and the aEEP reaches levels of 40% within 45° from boresight. This warrants a full EM simulation. At 110 and 350 MHz, the other two frequencies assessed in [13], the agreement between the IEP and aEEP is much better across the boresight angle range considered (up to 45°). However, the results still show a number of boresight angle where a similar requirement as for LOFAR would only be marginally satisfied with differences at the 3% level. It thus seems necessary to calculate the aEEP for the SKA-LOW stations to achieve the desired level of flux calibration reproducibility.

4 Conclusions

In this paper, I assessed the need for accurate modelling of individual EEPs in large, distributed aperture arrays like LOFAR and SKA-LOW. Although using an average EEP in station calibration causes a bias in the calibration solutions, this effect in itself does not seem to pose unacceptable degradation of system performance. However, station calibration should not worsen system performance (for this reason, LOFAR uses fixed station calibration tables for significant periods (few months) of time) and one should ensure that the combination of EEP modelling errors and source modelling errors together still gives acceptable results. For flux calibration transfer, knowledge of the average EEP is sufficient. The average EEP cannot be replaced by the isolated element pattern as that would give rise to unacceptably poor flux calibration reproducibility in many scenarios.

5 Acknowledgements

This work was supported by the Netherlands Organisation for Scientific Research. The author would like to thank Mark Waterson, Daniel Hayden, Maria Grazia Labate and Robert Laing for the in-depth discussion on the practical impact of station calibration, Pietro Bolli for providing the EEPs for a SKALA4AL station and Reinout van Weeren for raising the issue of flux calibration transfer from one field to another.

References

[1] M. P. van Haarlem *et al.*, "LOFAR: The Low Frequency Array," *Astronomy & Astrophysics*, vol. 556, no. A2, pp. 1–53, Aug. 2013.

[2] P. E. Dewdney, P. J. Hall, R. T. Schilizzi, and T. J. L. W. Lazio, "The Square Kilometre Array," *Proceedings of the IEEE*, vol. 97, no. 8, pp. 1482–1496, Aug. 2009.

[3] S. J. Wijnholds, S. van der Tol, R. Nijboer, and A. J. van der Veen, "Calibration challenges for future radio telescopes," *IEEE Signal Processing Magazine*, vol. 27, no. 1, pp. 30–42, Jan. 2010.

[4] G. Virone *et al.*, "Strong Mutual Coupling Effects on LOFAR: Modeling and In-Situ Validation," *IEEE Transactions on Antennas and Propagation*, vol. 66, no. 5, pp. 2581–2588, May 2018.

[5] S. J. Wijnholds, M. Arts, P. Bolli, P. Di Ninni, and G. Virone, "Using Embedded Element Patterns to Improve Aperture Array Calibration," in *International Conference on Electromagnetics in Advanced Applications*, Granada, Spain, 9 – 13 Sep. 2019.

[6] B. D. Jeffs *et al.*, "Signal Processing for Phased Array Feeds in Radio Astronomical Telescopes," *IEEE Journal of Selected Topics in Signal Processing*, vol. 2, no. 5, pp. 635–646, Oct. 2008.

[7] C. Haslam, C. Salter, H. Stoffel, and W. Wilson, "A 408 MHz all-sky continuum survey II - The atlas of contour maps," *Astronomy & Astrophysics Supplement Series*, vol. 47, pp. 1–2, 4–51, 53–142, Jan. 1982.

[8] G. Virone, F. Paonessa, L. Ciorba, and P. Bolli, "Results on UAV measurements," in *SKA-LOW Station Calibration Task meeting*, Florence, Italy, 1 – 3 Jul. 2019.

[9] K. Iheanetu *et al.*, "Primary beam effects in radio astronomy antennas - I. Modelling of the Karl G. Jansky Very Large Array (VLA) L-band beam using holography," *Monthly Notices of the Royal Astronomical Society*, vol. 485, no. 3, pp. 4107–4121, May 2019.

[10] S. Yatawatta *et al.*, "Initial deep LOFAR observations of the epoch of reionization windows – I. The north celestial pole," *Astronomy & Astrophysics*, vol. 550, no. A136, pp. 1–17, 2013.

[11] T. W. Shimwell *et al.*, "The LOFAR Two-metre Sky Survey - I. Survey description and preliminary data release," *Astronomy & Astrophysics*, vol. 598, no. A104, pp. 1–22, Feb. 2017.

[12] P. Di Ninni *et al.*, "Electromagnetic analysis and experimental validation of the LOFAR radiation patterns," *International Journal of Antennas and Propagation*, vol. 2019, no. 9191580, pp. 1–12, Jan. 2019.

[13] P. Di Ninni, M. Bercigli, P. Bolli, G. Virone, and S. J. Wijnholds, "Mutual Coupling Analysis for a SKA1-LOW Station," in *European Conference on Antennas and Propagation (EuCAP)*, Krakow, Poland, 31 Mar. – 5 Apr. 2019.